Using a climate-dependent model to predict mosquito abundance: Application to Aedes (Stegomyia) africanus and Aedes (Diceromyia) furcifer (Diptera: Culicidae)

Brigitte Schaeffer, Bernard Mondet, Suzanne Touzeau

Available online at www.sciencedirect.com
ScienceDirect
Infection, Genetics and Evolution 8 (2008) 422–432
Infection, Genetics and Evolution
www.elsevier.com/locate/meegid

Using a climate-dependent model to predict mosquito abundance: Application to *Aedes* (*Stegomyia*) *africanus* and *Aedes* (*Diceromyia*) *furcifer* (Diptera: Culicidae)

Brigitte Schaeffer [a,*], Bernard Mondet [b], Suzanne Touzeau [a]

[a] *INRA, UR341 Mathématiques et Informatique Appliquées, F-78350 Jouy-en-Josas Cedex, France*
[b] *Institut Français de Pondichéry, CP 33, 11 Saint-Louis Street, Pondicherry 605001, India*

Received 15 February 2007; received in revised form 2 July 2007; accepted 5 July 2007
Available online 10 July 2007

Abstract

Mosquitoes, acting as vectors, are involved in the transmission of viruses. Thus, their abundances, which strongly depend on the weather and environment, are closely linked to major disease outbreaks. The aim of this paper is to provide a tool to predict vector abundance.

In order to describe the dynamics of mosquito populations, we developed a matrix model integrating climate fluctuations. The population is structured in five stages: two egg stages (immature and mature), one larval stage and two female flying stages (nulliparous and parous). The water availability in breeding sites was considered as the main environmental factor affecting the mosquito life-cycle. Thus, the model represents the evolution of the mosquito abundance in each stage over time, in connection with water availability.

The model was used to simulate the abundance trends over 3 years of two mosquito species, *Aedes africanus* (Theobald) and *Aedes furcifer* (Edwards), vectors of the yellow fever virus in Ivory Coast. As both these species breed in tree holes, the water dynamics in the tree hole was reproduced from daily rainfall data. The results we obtained showed a good match between the simulated populations and the field data over the time period considered.

Keywords: Mosquito vector population; Mathematical model; Climate dependency

1. Introduction

Yellow fever, a vector-borne disease, remains a major public health problem both in Africa and South America. It is due to infection by a Flavivirus and causes a viral hemorrhagic fever in humans responsible for 30,000 deaths annually (Tomori, 2004). Furthermore, global warming may increase the outbreak risk of such infectious diseases associated with hot weather or rainfall pattern modifications. Chevalier et al. (2004) showed that geographical distributions of several arthropod-borne zoonoses have dramatically expanded over the last years. Although one knows that climate influences the abundance of vectors, it is still difficult to appreciate the effect of climate variations on the emergence and re-emergence of arbovirus diseases. That is mainly because the epidemiological process is driven by numerous tangled mechanisms, making analyses fairly complex. Breaking up the process and focusing on its different elements, in particular on the biology of the vectors which is the key of the virus transmission, might help to apprehend the global process.

Mathematical models combined with computer simulations are powerful tools for describing and understanding complex biological phenomena. Indeed, modelling allows to test assumptions, explain some events, or compare alternate strategies in decision-making. Thus, models have been widely used for studying complex biological processes such as population dynamics (e.g. Jarry et al., 1996; Ghosh and Pugliese, 2004; Awerbuch-Friedlander et al., 2005; Mazaris and Matsinos, 2006). For mosquito populations in particular, Moon (1976) developed a dynamic model, but that model did not consider environmental factors. Focks et al. (1993) proposed a dynamic life table model for *Aedes aegypti* taking

* Corresponding author at: INRA, Unité de Mathématiques & Informatique Appliquées, Centre de Recherche de Jouy-en-Josas, 78352 Jouy-en-Josas Cedex, France. Tel.: +33 1 34 65 22 18; fax: +33 1 34 65 22 17.
E-mail address: Brigitte.Schaeffer@jouy.inra.fr (B. Schaeffer).

1567-1348/$ – see front matter
doi:10.1016/j.meegid.2007.07.002

into account numerous variables, but lacking flexibility to be generalized to other species. Fouque and Baumgartner (1996) constructed a distributed delay model taking into account only part of the life-cycle of the *Aedes vexans* mosquito, from newly hatched larvae to emerging adults. Ahumada et al. (2004) built a population dynamics matrix model, taking into account temperature and rainfall. These authors obtained encouraging results because their model captured field data quite adequately. However, they acknowledged the importance of breeding site availability which they had not explicitly modelled. Shone et al. (2006) investigated the role of weather on mosquito species using statistical regression models. From this point of view, the dynamical aspect of abundance fluctuations is difficult to appreciate. In an epidemiological context, most studies did not take into account the vector population dynamics and set this population size to a constant value (Esteva and Vargas, 1999; Ngwa and Shu, 2000; Derouich et al., 2003; Ishikawa et al., 2003; Ngwa, 2004). As the necessity of taking into account the fluctuations of the vector density has been shown (Costantino et al., 1998; Chattopadhyay et al., 2004) the influence of the seasonality was sometimes introduced as a sinusoid function in the epidemiological model to roughly describe the mosquito population dynamics (Lord, 2004; Glass, 2005). In order to reproduce as best as possible the dynamics of a vector in its own environment, simulation models were developed (Focks et al., 1993; Depinay et al., 2004). These models include numerous parameters that could be difficult to apprehend in field conditions, such as nutrient competition for example. Validating such models might prove difficult, as sensitive parameters, if not well estimated, might distort the model outputs.

In the present paper, our approach was to develop a model as simple and generic as possible to investigate the mosquito population dynamics, taking into account only the most relevant steps of the mosquito life-cycle and the most influent environmental factors. Such a model aims at capturing the major trends of the mosquito population size along time. Moreover, this model could easily be integrated in a larger modelling process which would, for example, include models of virus development and host demography.

This paper is divided into three major sections. The first one presents the generic model based on the life-cycle graph of a mosquito population. The second section shows how environmental factors are integrated into the model. The third section describes an application of the model using data from yellow fever vectors, *Aedes* (*Stegomya*) *africanus* and *Aedes* (*Dicermomya*) *furcifer*, in West Africa (Mondet, 1994, 1997); parameters were estimated and a sensitivity analysis was performed. Finally, conclusions are drawn.

2. The generic population model

To represent the dynamics of the mosquito population and the climate influence, we chose a matrix framework (Caswell, 2001) that is commonly used to study the dynamics of structured populations (Jensen, 1995; Jarry et al., 1996; Bommarco, 2001; Choi and Ryoo, 2003; Thomas et al., 2005). Moreover, this discrete time step corresponds well to the nature of the field data. In this section, we first present the mosquito life-cycle. Then we describe the death, growth and reproduction processes that will be finally merged to produce the population dynamic model.

2.1. The mosquito life-cycle

The biological cycle of the mosquito is represented in Fig. 1. The *Aedes* females lay their eggs on the limits of stagnant waters in their breeding sites. These eggs hatch when they are flooded. The aquatic larvae, resulting from eggs, pass through four stages of development. The last molt leads to a flying adult, winged, male or female. As soon as female mosquitoes emerge, they are fertilized, mating occurring only once in their lifetime. Then females need to find a blood meal host to start a gonotrophic cycle. When the cycle is over, female mosquitoes will deposit their eggs. After laying, females need a new blood meal to start a new gonotrophic cycle, and so on until they die. A female generally goes through 5–7 cycles.

The population model we built takes into account only females because males are not involved in transmission disease. The model is based on the three phases of the mosquito life-cycle: the eggs, the aquatic forms and the adults who produce the eggs. To describe the maturation of eggs, we took into account two egg stages: an immature stage denoted $w1$, followed by a mature stage denoted $w2$ from which eggs can hatch. The transition between these two stages may be controlled by climate. Then, we considered one larval stage, denoted L, corresponding to the aquatic forms that include instars (1 to 4) and pupae. Right after emergence as aerial adults females enter the nulliparous stage denoted A_1 during which they are fertilized and at the end of which they lay their first eggs. Right after this first laying, they enter the parous stage denoted A_2 during which they go through several more layings. The availability of hosts which provide blood meals and hence govern the laying, was not considered as a limiting factor and so, was not included in the model.

Consequently, our mosquito population is structured in five stages, $w1$, $w2$, L, A_1 and A_2, and we chose a discrete time

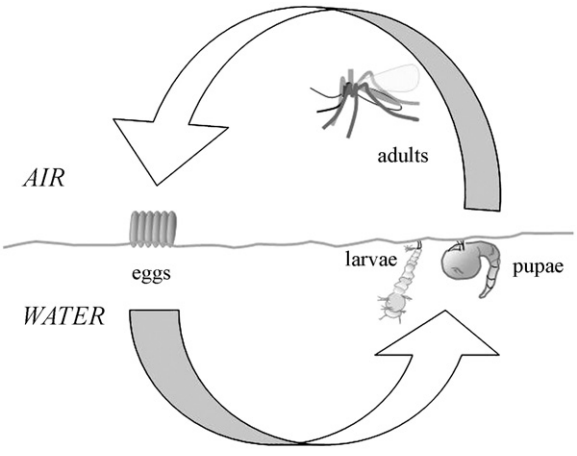

Fig. 1. Biological cycle of mosquitoes.

process to represent its dynamic over time. So at each time t, the population is described by its state vector denoted N_t,

$$N_t = \begin{pmatrix} w1_t \\ w2_t \\ L_t \\ A_{1_t} \\ A_{2_t} \end{pmatrix}.$$

To express the evolution of the population with time, we modelled the processes that affect the abundances of stages i, $i \in \{w1, w2, L, A_1, A_2\}$, during each time step. These processes are represented in the life-cycle graph in Fig. 2: birth, maturing from stage to stage, and death. The following paragraphs present these three processes (in reverse order to simplify the understanding of the model) and then, the resulting population dynamic model.

2.2. Death

Death can occur throughout the life of the mosquito. For each stage i, the mortality rate is denoted $q_{i\mathrm{D}}$ and is defined as the proportion of individuals in stage i that die during each time step.

2.3. Growth

For any stages i and j, $(i, j \in \{w1, w2, L, A_1, A_2\})$, the transition rate from stage i to stage j is denoted q_{ij}, and is defined as the proportion of individuals in stage i at time t that move (or stay) into stage j (or i) at time $t + 1$. As the population is considered to be closed (no migrations), one can write for each stage i:

$$\sum_{j \in \{w1, w2, L, A_1, A_2\}} q_{ij} + q_{i\mathrm{D}} = 1.$$

The residence times which correspond to the development time in each stage are not identical; for instance, the larval stage L can last from 6 to 20 days whereas the parous adult stage, A_2, can be up to 30 days. The time step needs to be chosen so as to be lower than the minimum residence time in any stage and the time unit is set to one time step ($\Delta t = 1$). In the following application, the time step is set to 1 day. Therefore, between two time steps, an individual can either remain in its current stage, or pass into the following stage, except for the A_2 stage, or die. In A_2 stage, an individual can only remain in its stage or die. For instance, for $i = L$, we have: $q_{Lw1} = q_{Lw2} = q_{LA_2} = 0$, hence $q_{LA_1} + q_{LL} + q_{L\mathrm{D}} = 1$. We assumed that the transition rate from stage i to next stage, in the absence of death, is equal to the inverse of the mean residence time in stage i, denoted T^i_{rsd}. It means that in the absence of death, the individuals would leave stage i with frequency $1/T^i_{\mathrm{rsd}}$. The underlying hypothesis is that the stage-duration distribution is geometric: the individual probability of moving from stage i to stage $i + 1$ is a constant, independent of the time spent in stage i. This hypothesis, though rather unrealistic in mosquito populations, is a very common simplification. Incorporating mortality, we apply this frequency to the fraction of the population in stage i that does not die during the time step. With $(1 - q_{i\mathrm{D}})$ as the survival rate for stage i, we obtain:

$$q_{ij} = \frac{1}{T^i_{\mathrm{rsd}}}[1 - q_{i\mathrm{D}}], \quad \text{if } j = i + 1, \text{ otherwise } q_{ij} = 0.$$

As $q_{ii} + \sum_{j \neq i} q_{ij} + q_{i\mathrm{D}} = 1$ we deduce that:

$$q_{ii} = \left(1 - \frac{1}{T^i_{\mathrm{rsd}}}\right)[1 - q_{i\mathrm{D}}].$$

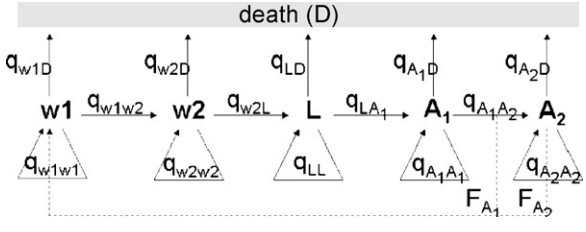

Fig. 2. Life-cycle graph of female mosquitoes. Nodes represent the stages: $w1$ = immature eggs, $w2$ = mature eggs, L = larval stages, A_1 = nulliparous adults, A_2 = parous adults. The q_{ij} $(i, j \in \{w1, w2, L, A_1, A_2\})$ are the transition rates, the $q_{i\mathrm{D}}$ are the mortality rates and the F_i, $i \in \{A_1, A_2\}$, are the fecundities. Each arrow represents a possible transition between two stages during a time step.

2.4. The reproduction process

Female mosquitoes lay eggs several times during their adult stage, each laying occurring after a blood meal. We assumed that the search for a blood meal host takes very little time compared to the model time step, so we neglected this delay. The transition from the nulliparous stage to the parous stage is triggered by the first laying. Let us denote T_{c}, with $T_{\mathrm{c}} \geq \Delta t$, the duration between the emergence and the first laying, which corresponds to the length of a gonotrophic cycle. Thus, at each time step, the transition rate from the nulliparous stage to the parous stage is expressed as:

$$q_{A_1A_2} = \frac{1}{T_{\mathrm{c}}}[1 - q_{A_1\mathrm{D}}].$$

As $q_{A_1A_1} + q_{A_1A_2} + q_{A_1\mathrm{D}} = 1$ we deduce that:

$$q_{A_1A_1} = \left(1 - \frac{1}{T_{\mathrm{c}}}\right)[1 - q_{A_1\mathrm{D}}].$$

Nulliparous females lay their eggs when they enter the parous stage. The number of females that pass into the parous stage is $q_{A_1A_2} \times A_1$. Let nwf be the mean number of female eggs produced by one female. Then the number of eggs produced at each time step by the nulliparous females is given by $\mathrm{nwf} \times q_{A_1A_2} \times A_1$. Hence the fecundity is

$$F_{A_1} = \frac{\mathrm{nwf} \times q_{A_1A_2} \times A_1}{A_1} = \mathrm{nwf} \times q_{A_1A_2}.$$

Parous females go through several gonotrophic cycles. As we neglected the delay induced by the search for a blood meal host, the time between two successive layings is equal to T_{c}, the length of a gonotrophic cycle. Thus, at each time step, the

proportion of parous females that lay their eggs and start a new cycle, denoted q_c, is given by:

$$q_c = \frac{1}{T_c}[1 - q_{A_2D}].$$

Hence, the number of eggs produced by parous females at each time step is:

$$\text{nwf} \times q_c \times A_2,$$

which gives the following expression for the fecundity of parous females:

$$F_{A_2} = \text{nwf} \times q_c.$$

2.5. The population dynamics

The q_{jD} (death), q_{ij} (growth) and F_i (reproduction) are the elements of the transition matrix, denoted Q, established from the life-cycle graph given in Fig. 2. Q is also called the population projection matrix associated to the model.

$$Q = \begin{Bmatrix} q_{w1w1} & 0 & 0 & F_{A_1} & F_{A_2} \\ q_{w1w2} & q_{w2w2} & 0 & 0 & 0 \\ 0 & q_{w2L} & q_{LL} & 0 & 0 \\ 0 & 0 & q_{LA_1} & q_{A_1A_1} & 0 \\ 0 & 0 & 0 & q_{A_1A_2} & q_{A_2A_2} \end{Bmatrix}.$$

We considered that the transition rates (each element of the matrix Q) could be affected by the climate conditions, so we say that Q is climate-dependent and we denote it Q_t. As no delay was incorporated in the model, the state of the mosquito population at time t, only depends on the population state at time $t-1$. Thus, on the current climate conditions:

$$N_{i,t} = Q_t \times N_{i,t-1}.$$

3. Climate dependency

Climatic factors acting on the development of the mosquito populations vary according to the characteristics of the weather. That is particularly true in areas were there is an alternation of seasons (cold and hot or dry and wet). Here we focused on the mosquito populations of tropical zones where dryness is the limiting factor but temperature is not. More precisely, we considered three steps in the mosquito development cycle for which the need of water is crucial: hatching, larva survival and for some species, maturation of eggs. Thus, we introduced in the model a water dependency, by considering the available water quantity in the breeding sites. Let us denote EP that quantity. EP depends on both the pluviometry and on the shape of the breeding sites. So EP needs to be determined for each species considering its specific environment.

3.1. Maturation of eggs

Once the mosquito eggs are deposited by the females, they go through a maturation period corresponding to $w1$. At the end of this period, eggs have acquired the potentiality of hatching and move to the $w2$ stage. Given that for some species, maturation requires a dry period, we introduced in the model the possibility of such a conditional transition from $w1$ to $w2$. We expressed that condition by adding to the corresponding transition rate, a steeply decreasing sigmoid function σ, that represents the egg maturation ability as a function of the trapped water ratio $\text{EP}/\text{EP}_{\max}$:

$$q_{w1w2,t} = \frac{1}{T^{w1}_{\text{rsd}}}(1 - q_{w1D})\sigma\left(\frac{\text{EP}_{t-1}}{\text{EP}_{\max}}\right).$$

As $q_{w1w1} + q_{w1w2} + q_{w1D} = 1$, the proportion of eggs that remains immature, q_{w1w1}, also depends on EP.

The sigmoid function is a simple S-shape function, with a steep slope for intermediate values, an almost flat shape for small values and a saturation level for higher values. It approximates a step function. This sigmoid function σ verifies the following conditions: when $\text{EP}_{t-1} = 0$, the surviving eggs leave stage $w1$ with frequency $1/T^{w1}_{\text{rsd}}$, and when $\text{EP}_{t-1} = \text{EP}_{\max}$, no more eggs move to stage $w2$. So:

$$\sigma\left(\frac{\text{EP}_{t-1}}{\text{EP}_{\max}}\right) = \frac{e^{-\theta_{w1.1}(\text{EP}_{t-1}/\text{EP}_{\max})^{\theta_{w1.2}}} - e^{-\theta_{w1.1}}}{1 - e^{-\theta_{w1.1}}}$$

with parameters $\theta_{w1.1} > 0$ and $\theta_{w1.2} > 0$.

3.2. Hatching

Eggs are laid by the females on the water edge. As the water level in the hole varies during the laying season, eggs are distributed along the cavity walls. Once eggs are mature, they can hatch if they are flooded. Hatching therefore depends on the trapped water quantity. Thus, we modulated the transition rate q_{w2L} by an increasing function of $\text{EP}/\text{EP}_{\max}$:

$$q_{w2L,t} = (1 - q_{w2D}), \qquad \theta_{w2.1}\left(\frac{\text{EP}_{t-1}}{\text{EP}_{\max}}\right)^{\theta_{w2.2}},$$

with parameters $\theta_{w2.1} > 0$ and $\theta_{w2.2} > 0$. So, when $\text{EP}_{t-1} = 0$, then $q_{w2L,t} = 0$ which means that no hatching occurs; when $\text{EP}_{t-1} = \text{EP}_{\max}$, then mature surviving eggs hatch at frequency $\theta_{w2.1}$ which corresponds to the inverse of the mean residence time in $w2$ stage, $1/T^{w2}_{\text{rsd}}$. We chose a power function to represent the climate dependency. Indeed, it is a quite flexible increasing function as it allows: quadratic-like curves when $\theta_{w2.2} > 1$, i.e. curves that increase more rapidly for higher values; or square-root-like curves when $0 < \theta_{w2.2} < 1$, i.e. curves that increase more rapidly for lower values.

3.3. Larva mortality

The main factor contributing to larva mortality is habitat desiccation. Because several studies showed a density-dependence of the larval survivorship (Renshaw et al., 1993; Lord, 1998; Teng and Apperson, 2000; Agnew et al., 2002), we also took into account the density effect by considering the available water by larva, EP/L. So, we expressed the larval mortality q_{LD} as a decreasing function of EP/L, $L \neq 0$, as

follows:

$$q_{LD,t} = q_{LDm} + (1 - q_{LDm})\, e^{-\theta_{L.1}(EP_{t-1}/L_{t-1})^{\theta_{L.2}}}$$

with $\theta_{L.1} > 0$, $\theta_{L.2} > 0$. When $EP_{t-1}/L_{t-1} = 0$, $L_{t-1} \neq 0$, then $q_{LD,t} = 1$ which means that all larvae die; and when EP_{t-1}/L_{t-1}, $L_{t-1} \neq 0$, increases, then $q_{LD,t}$ declines to q_{LDm} which is the minimal mortality rate for the larvae. When there are no larvae, $L = 0$, there are no larvae dying whatever the mortality rate applied. When $L \to 0$, $q_{LD} \to Q_{LDm}$. So for $L = 0$ we set $q_{LD} = q_{LDm}$. In this case, the climate dependency is based on an exponential function, as we assumed that the decrease would be rather steep.

4. Application

We applied the mosquito population model with climate dependency to two specific populations of yellow fever vectors, *Aedes africanus* and *Aedes furcifer* (Cordellier, 1978), which live in forest galleries and in the bordering savannahs in Ivory Coast. Their blood meal hosts are primates and humans. Both mosquito species are active when primates rest in the canopy. They can also leave the canopy and bite humans who come into the forest. Moreover, *A. furcifer* is capable of entering neighbouring villages. This close proximity of both species to their blood meal hosts supports our assumption that the time needed to find a host is negligible compared to the 1-day time step.

Our aim was to reproduce the major trends in the mosquito population abundances, comparing the simulations of the model with field data. To run the model, we had to determine the dynamics of the trapped water, EP_t, and the parameters values. EP_t is strongly related to the type of the habitat and so a specific habitat model was developed. Concerning the parameter values, we assumed that the biological characteristics were known, and we estimated the remaining parameters. With these parameters, simulations were produced by running the generic population model with the specific habitat model. In this section, we successively present the field data, the specific habitat modeling, the parameters, and then, simulations and results. Following that, we include a sensitivity analysis to estimate the contribution of the different parameters to the variability of the model. Then we close this part with a short discussion.

4.1. Field data

Over a 3-year period, Mondet (1994) studied the abundance of mosquito vectors of yellow fever in the Dezidougou area, Ivory Coast, after a serious outbreak of yellow fever in 1982. The village of Dezidougou is located at the limit of the forest and the savannah. In that zone, the climate is divided into two seasons: a dry season lasting from November to April and a wet season with two peaks of rain. In the rainy season, the temperature is rather uniform, with a minimum ranging between 21 and 25 °C and a maximum ranging between 25 and 27 °C. From the first rains, relative humidity reaches a maximum ranging between 95 and 100% and persisting during all the rainy season. Daily rainfall was recorded in Dezidougou from January 1989 to December 1991. Over these 3 years, female mosquitoes were captured every day during a 1-week period, using yellow fever vaccinated human baits spread over 9 sites from 5 to 8 p.m. There was a 30-day interval between the captures during the first 2 years and a 40-day interval the third year. Among the species collected, *A. africanus* and *A. furcifer*, were well represented. Each month, a mean daily abundance was calculated for these two species. These abundances are given by the bars in Fig. 7 with the simulation results.

4.2. Specific habitat modelling

Breeding sites of both populations, *A. africanus* and *A. furcifer*, are tree holes of variable capacities supplied with rainwater. During each rainfall, the rainwater that streams is trapped until saturation of the tree holes. We considered a tree hole as a cone. Let us denote EP_{max} the maximal capacity of the tree hole, $\pi \times R^2$ its basis and H its height (Fig. 3a). Then, EP_{max} is equal to:

$$EP_{max} = \pi \times R^2 \times \frac{H}{3}.$$

Let EP_{t-1} be the trapped water in the cone at time $t-1$. The radius of the water surface at time $t-1$ is:

$$r_{t-1} = \sqrt[3]{K\frac{3EP_{t-1}}{\pi}}, \quad \text{where } K = \frac{R}{H}.$$

The water surface at time $t-1$ is: $S_{t-1} = \pi(r_{t-1})^2$.

To determine the trapped water at time t, we need to consider both rainfall and evaporation that take place during the time step. We first consider evaporation (Fig. 3a and b) that is related to the surface of the water S. The larger S is, the greater the evaporation. So we express the proportion of water evaporated between time $t-1$ and t, denoted $\theta_{evap,t}$, as an increasing function of S_{t-1}:

$$\theta_{evap,t} = 1 - e^{-\rho_{evap} S_{t-1}}, \quad \text{with } \rho_{evap} \geq 0.$$

Then, we introduce the rainfall. Let P_t be the height of the rainfall between time $t-1$ and time t. The volume of the rainfall getting into the cone is approximated by a cylinder of

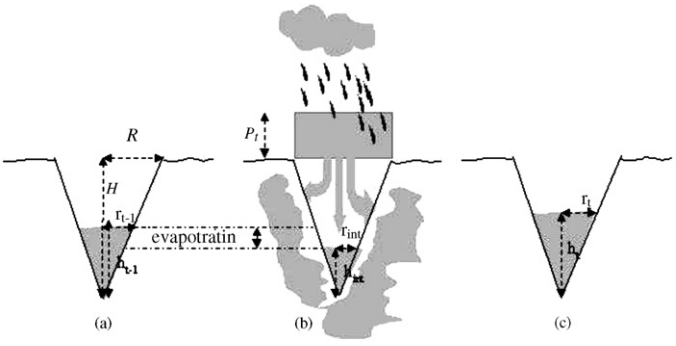

Fig. 3. Successive phases of the tree-hole filling up process: evaporation and rainwater trapping between time $t-1$ and time t. (a) Time $t-1$, (b) between evaporation and rainwater trapping and (c) time t.

basis $\pi \times R^2$ and height P_t (Fig. 3b and c). At this point, we have to take into account the part of this rainwater that seeps through the walls. The more the hole is filled, the less infiltration occurs. Thus, we express the fraction of the rain effectively trapped in the tree hole, denoted $\theta_{\text{eff},t}$, as a decreasing function of the difference between the basis of the cone and the surface of the water trapped in the cone after evaporation. We denote $\Delta S_{t-1,t}$ that difference. So we have:

$$\theta_{\text{eff},t} = \mathrm{e}^{-\rho_{\text{eff}}\,\Delta S_{t-1,t}}, \quad \text{with } \rho_{\text{eff}} > 0.$$

Taking into account the fact that EP is bounded by $\text{EP}_{\max}$, then EP_t, the trapped water at time t, is given by:

$$\text{EP}_t = \min((\text{EP}_{t-1}(1-\theta_{\text{evap},t}) + \theta_{\text{eff},t}\pi R^2 P_t), \text{EP}_{\max})$$

Combining this trapped water dynamics with the generic population model, we obtain a fully defined tree-hole breeding mosquito model.

4.3. Parameters

The biological characteristics of the two mosquito species are given in Table 1. These biological features are averages coming from references of the literature, biological surveys or expert advice. We also fixed the size of the cone-shaped tree hole, the depth being equal to 80 mm and radius to 30 mm, for both species. The resulting capacity is 75 ml which is a reasonable value for a tree hole. The remaining parameters of the model, i.e. the parameters related to the climate influence, were estimated from the field data.

4.4. Simulations and parameter estimation

To run the tree-hole breeding mosquito model we used the parameters described in Table 1 and the rainfall data from the Dezidougou area. We set the initial conditions: at time 0, we considered that there were only immature eggs in the tree hole, and we fixed that number $w1_0$ to 10 eggs. So $N_0 = (w1_0, 0, 0, 0, 0)$, with $w1_0 = 10$. We set the time step to 1 day. We then had to estimate the climate-dependent parameters. Comparing the simulated mosquito abundances with field data gathered over the first 2 years, i.e. from January 1989 to December 1990, we estimated the optimal values for these parameters by minimizing a least square criterion. A scaling was needed for this fit: abundance data represent a mean daily number of mosquitoes caught on a given area, whereas the simulations reproduce the daily number of female mosquitoes breeding in a given tree hole. We then simulated a third year using the estimated parameters. The third year of mosquito abundance data was hence used only to validate the model. All simulations were performed using the R software.

Table 2
Parameters of the model estimated from observed data over 1989–1990

Parameters of the model	*Aedes africanus*	*Aedes furcifer*
ρ_{evap}	0.00005	0.00004
ρ_{eff}	2.27	1.61
$\theta_{w1.1}$	–	15.7
$\theta_{w1.2}$	–	0.86
$\theta_{w2.1}$	0.03	0.06
$\theta_{w2.1}$	0.67	5.90
$\theta_{L.1}$	0.25	1.96
$\theta_{L.2}$	0.28	0.07

ρ_{evap} and ρ_{eff} concern, respectively, the evaporation and the filling of the tree hole. The θ_x parameters are related to the influence of climate on mosquito development at three ages: immature eggs ($x = w1$), mature eggs ($x = w2$), larvae ($x = L$).

4.5. Results

Simulations were produced by running the model over the 3 years, using the parameter values in Table 1 and the estimated parameters given in Table 2.

The first estimated parameters ρ_{evap} and ρ_{eff}, related to the filling of the tree hole are, respectively, involved in the

Table 1
Biological characteristics and simulation parameters introduced in the model

	Parameters	*Aedes africanus*	*Aedes furcifer*
Biological characteristics			
Residence time in $w1$ stage (days)	T^{w1}_{rsd}	7	7
Mortality rate in $w1$ stage	$q_{w1\text{D}}$	0.05	0.01
Mortality rate in $w2$ stage	$q_{w2\text{D}}$	0.05	0.01
Residence time in L stage (days)	T^{L}_{rsd}	12	16
Minimal mortality rate in L stage	$q_{L\text{Dm}}$	0.05	0.01
Cycle length between two layings (days)	T_{c}	7	7
Mortality rate in A_1 stage	$q_{A_1\text{D}}$	0.05	0.01
Mortality rate in A_2 stage	$q_{A_2\text{D}}$	0.15	0.06
Number of female eggs/female	nwf	40	30
Habitat characteristics			
Tree hole depth (mm)	H	80	80
Radius of the tree hole basis (mm)	R	30	30
Simulation conditions			
Initial population (at time $t = 0$)	N_0	(10, 0, 0, 0, 0)	(10, 0, 0, 0, 0)
Time step (days)	Δt	1	1

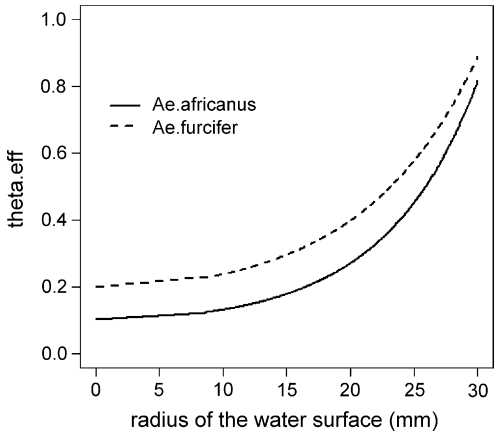

Fig. 4. Efficient fraction of rainfall θ_{eff} in function of the radius of the trapped water surface r for each species.

expression of θ_{evap} and θ_{eff}. We note that the evaporation rates θ_{evap} are very similar for both species and never exceed 0.2, which is usual in forest area. The efficient fraction of rainfall θ_{eff} expressed in function of the water surface in the holes is slightly higher for *A. furcifer* than for *A. africanus*, as shown in Fig. 4. Consequently, the trapped water dynamics represented in Fig. 5 are a little different in the two breeding sites.

The parameters in Table 2 related to the climate influence on the transition rates are different between the two mosquito species. Consequently, the impact of the trapped water EP on these transition rates also differs between the two species, as shown in Fig. 6. For the egg maturation, no trapped water effect was introduced for *A. africanus* (Fig. 6a). However, for *A. furcifer*, the maturation rate rapidly decreases when the tree hole fills in Fig. 6b. The hatching rate increases with EP for both

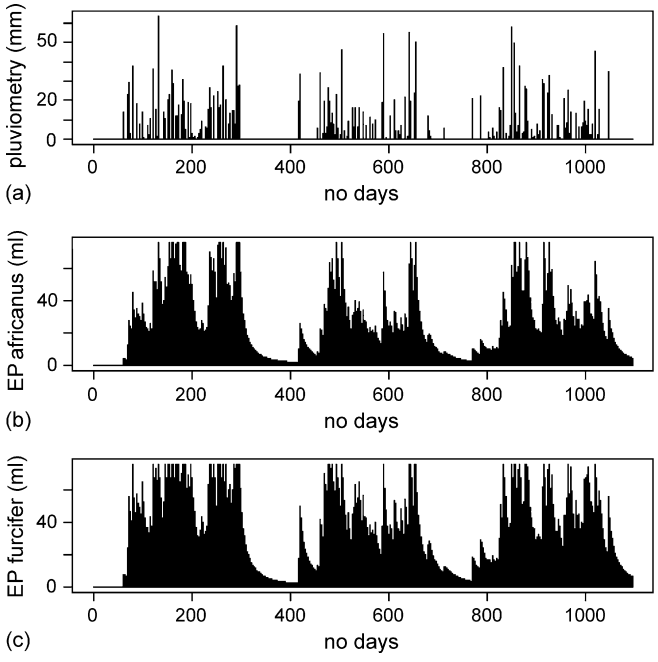

Fig. 5. (a) Pluviometry in Dezidougou from January 1989 to December 1991; and related trapped water (EP) dynamics in the cone-shaped tree hole of (b) *Aedes africanus* and (c) *Aedes furcifer*.

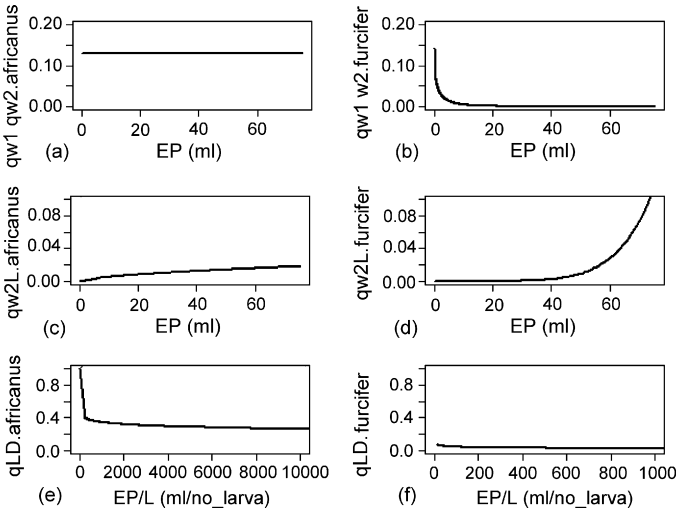

Fig. 6. Climate-dependent transition rates as functions of the tree hole trapped water EP (a–d) or trapped water available by larva EP/L (e and f): (a and b) immature to mature egg transition rates, (c and d) hatching rates, (e and f) larva mortality. The graphs on the left correspond to *Aedes africanus* (a, c and e); the graphs on the right to *Aedes furcifer* (b, d and f).

species. For *A. furcifer* the growth starts for higher levels of EP, but the increase is then steeper than for *A. africanus* (Fig. 6c and d). The *A. furcifer* larva mortality is almost always to its minimal value q_{LDm} (Fig. 6f): neither the trapped water quantity, nor the larva density have much impact on this value. The *A. africanus* larva mortality shows a stronger density dependence: the larva mortality decreases with the trapped water available by larva.

The mosquito abundance data and simulations are represented in Fig. 7. Note that the scales of the two graphics are different, as *Ae. africanus* is globally twice as abundant as *Ae. furcifer*. The estimation was performed over the first 2 years and the resulting abundances fit the field data well. Simulations over the third year correspond to predictions: for both species we notice an overestimate. Graphs in Fig. 7 show that the abundance fluctuations of both mosquito species roughly follow the fluctuations of the trapped water in the tree holes

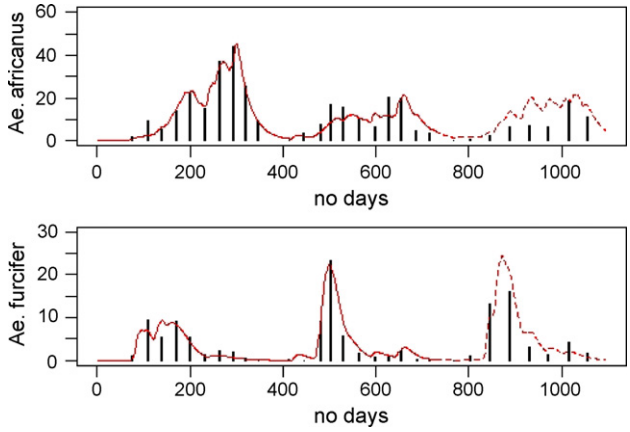

Fig. 7. Abundance of *Aedes africanus* and *Aedes furcifer* female adults ($A_1 + A_2$). The bars correspond to the number of adult mosquitoes caught in a day in Dezidougou (average over a week calculated once a month). The lines represent the simulation results: solid lines correspond to the fitted abundances and dashed lines correspond to the predictions.

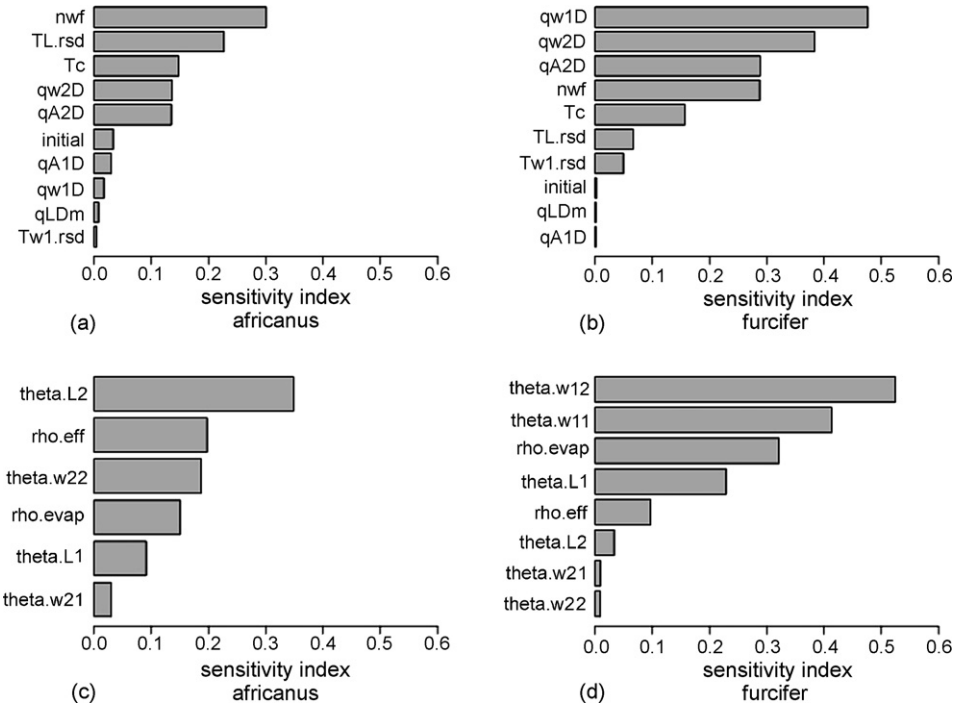

Fig. 8. Sensitivity indexes of the biological parameters and the initial egg population (a and b) and the estimated parameters (c and d). Graphics (a and c) concern *Ae. africanus*, graphics (b and d) concern *Ae. furcifer*. The sensitivity indexes were obtained after a ±20% variation of the reference values shown in Table 1 (for a and b) and in Table 2 (for c and d).

(Fig. 5). However, the abundance peaks of the two species are shifted in time. The population of *A. africanus* increases along the rainy season whereas the population of *A. furcifer* rises at the beginning of the rainy season then declines. Moreover, the amplitude of the abundance fluctuations is higher for *A. africanus* than for *A. furcifer*.

4.6. Sensitivity analysis

To determine which parameters have the greatest impact on the model, we carried out a sensitivity analysis on the biological characteristics, the initial number of eggs and the estimated parameters. Because the biological characteristics are needed to estimate the remaining parameters, we performed two separate analyses. In both cases, parameters were increased and decreased by 20% from their reference values given in Tables 1 and 2. To explore this parameter space, we used a complete experimental design. The output variable, denoted Y, corresponds to the distance between the simulated abundances $A = A_1 + A_2$ and the field data O, calculated at the observation times t_o as follows:

$$Y = \sum_{t_o} \left(\frac{A_{t_o} - O_{t_o}}{O_{t_o}} \right)^2.$$

The sensitivity index is defined for each parameter i by:

$$S_i = \frac{V(Y) - V_{-i}}{V(Y)}$$

where $V(Y)$ is the total variance and V_{-i} is the sum of all variance terms that do not include the parameter i. The higher the index, the more influence the parameter has. The results are given by the barplots in Fig. 8.

Globally, the *A. furcifer* model is more sensitive to parameter variations than the *A. africanus* model. For both species, the mean number of female eggs produced by one female, the mortality rates in the $w2$ and A_2 stages and the cycle length between two layings have a major impact on the model output. The residence time in the L stage specifically affects the *A. africanus* model, whereas the mortality in the $w1$ stage only affects the *A. furcifer* model. The other biological parameters and the initial condition do not show a great influence.

For both species, the estimated parameters related to the trapped water dynamics show a moderate influence on the model outputs. $\theta_{w1.1}$ and $\theta_{w1.2}$, involved in the maturation of *A. furcifer* eggs, have a high sensitivity index. θ_{L2} involved in the larva mortality has the most impact on the *A. africanus* model whereas it does not affect the *A. furcifer* model; in this latter model, θ_{L1} has a moderate influence.

These additional simulations and the analyses were performed using the R software.

4.7. Discussion

The model we developed for the *A. africanus* and *A. furcifer* in Ivory Coast was able to reproduce the major trends in the adult population abundances. The third simulation year, which was predicted from parameters estimated over the first 2 years, did not show such a good fit. It caught the global patterns but overestimated the abundances, both for *A. africanus* and *A. furcifer*. Many explanations may hold: one could think that because of a lower capture frequency the third year, field data

did not catch the abundance peaks, or that the mosquitoes that year experienced a mortality increase ....

For both species, the most influent parameters are those that relate to the production and survival of eggs. However, the initial condition has very little impact, which implies that the population development does not only depend on the egg survival from the previous rainy season. Each year, the abundances of each species show a distinct pattern. These different trends are explained by the fact that the eggs of *A. furcifer* need a dry season to mature: eggs laid during the rainy season become mature during the next dry season and are therefore accumulated in this stage, until new rainfalls. The sensitivity analysis showed that this maturation process is critical in the population development. The very low larva mortality rate obtained for *A. furcifer* suggests that the larvae need very little water to survive. Therefore, once the larvae hatch, which only occurs when sufficient water is available in the tree hole, they are quite resilient to environmental fluctuations. *A. africanus* larvae seem to be more affected by larva density and water availability, which is supported by the sensitivity analysis (θ_{L2} has a high index). It could explain why the adult abundance fluctuations observed seem to follow more closely the trapped water evolution.

No field data were available to define the tree holes. From expert advice we chose a conical shape as one of the simplest representation of a rather deep and narrow hole. Moreover, we were able to fix the hole capacity to a reasonable value (75 ml). Keeping the same fixed capacity and varying the shape of the cone (width and depth), the results were not modified. The only differences observed were the estimations of the parameters controlling the filling of the tree hole, ρ_{evap} and ρ_{eff}, which fluctuated slightly. These two parameters have a moderate impact on the adult population abundances. However, ρ_{eff} has different values for both species, which leads us to assume that t may not have the same type of breeding sites. The retention of rainwater in the tree hole appears higher for *A. furcifer*: it could be due to a different shape of the tree hole or a different species of tree. Indeed, various types of breeding sites are available in the wild and mosquitoes might show preferences. It is the case for *Aedes usambara*, vector of the Chikungunya virus, which was caught inside bamboo plantations in Ivory Coast (Mondet and Montange, 1993). So to simulate the abundance of *A. usambara*, we would have to consider the breeding habitat as a cylinder-shaped hole to represent the EP process.

Our results suggest that the field populations of *A. africanus* and *A. furcifer* are well simulated by a stage-structured matrix model incorporating pluviometry influence. In that area, as far as we know, pluviometry is the only environmental limiting factor in the *Aedes* population development. Other factors, such as temperature, are not considered as limiting factors for both species in that area, and thus were not introduced in the model. However, they may also interact with pluviometry and modulate the mosquito population abundance. Nevertheless, this simple pluviometry-based model allowed us to capture the major trends in the population fluctuations, which was our aim in this application.

In Dezidougou the yellow fever is not endemic. The virus migrates from the southern forests during the rainy season, carried by primate and mosquito populations along the forest galleries. So the virus usually appears in savannah at the end of the rainy season. Both data and model agree on the following trend: the population of *A. africanus* is higher at the end of the rainy season whereas the population of *A. furcifer* shows a peak at the beginning of the season. Therefore, high *A. africanus* abundances increase the risk of a yellow fever epidemic in the monkey population of the Dezidougou area. But YF virus can survive in some *A. furcifer* eggs during the dry season. These females born of contaminated eggs will be capable to generate a human YF outbreak at the beginning of the following rainy season, especially with abundant rainfalls that lead to a high peak of *A. furcifer*.

5. Conclusions

We have presented a generic mosquito population model that includes several features: various development stages, climate and density dependency. Results obtained by applying the model to field data have shown that it allows a rather good assessment of the mosquito abundance trends. Indeed, by taking into account the rain profile in the demographic process, we have reproduced over 2 years, and predicted over 1 year, the population evolution of two species of mosquitoes, that differ by their ecological and biological features. The model fitted the data quite accurately during the first 2 years; it overestimated the abundances the third year, but reproduced the global patterns. In this deterministic model, pluviometry fluctuations were sufficient to capture the major trends in the population abundances. However, we may introduce stochastic factors to account for the biological variability. As we introduced the effect of trapped water, which is the main factor under inter-tropical climates for tree-hole breeding mosquitoes, we can also introduce other factors, such as the temperature for example. We can also reduce or expand the number of stages. Although, the generic nature of the model allows the incorporation of many other factors, we have to keep in mind the parsimony rule before refining the model.

Applying the model to real abundance and rainfall data, we have shown its predictive capacity once parameters are estimated. Therefore, this model could prove useful to estimate the abundance evolution of disease vectors, according to different climate change scenarios. Thus, such a model is a valuable tool to assess the risk of an epidemiological outbreak.

Appendix A. Filling up process of the tree hole

Let us consider a tree hole as an inverted cone with πR^2 its basis and H its depth.

At each time step, the rainwater trapped in the tree hole, EP_t is updated. The filling up process is composed of two successive phases: evaporation and rainwater trapping (Fig. 3).

The volume of the water that evaporates between $t-1$ and t is $\theta_{\text{evap},t} \times \text{EP}_{t-1}$, where $\theta_{\text{evap},t}$ is the evaporation rate. This rate depends on the water surface at $t-1$, $S_{t-1} = \pi r_{t-1}^2$. The

larger S_{t-1}, the greater the evaporation. Moreover, $\theta_{\text{evap},t}$ being a fraction, it is bounded between 0 and 1. So we express the evaporation rate, $\theta_{\text{evap},t}$, between time $t-1$ and time t as $\theta_{\text{evap},t} = 1 - e^{-\rho_{\text{evap}} S_{t-1}}$, with $\rho_{\text{evap}} \geq 0$.

Let us denote EP_{int} the trapped water quantity remaining in the tree hole after the evaporation process is applied between $t-1$ and t:

$$\text{EP}_{\text{int}} = \text{EP}_{t-1}(1 - e^{-\rho_{\text{evap}} S_{t-1}}).$$

This volume can also be expressed as $\text{EP}_{\text{int}} = (1/3)\pi r_{\text{int}}^2 h_{\text{int}}$ where r_{int} and h_{int} are, respectively, the radius and the height of the water remaining in the hole.

Let us fix $K = R/H$. Using the cone property $R/H = r_{\text{int}}/h_{\text{int}}$ we can write that:

$$\text{EP}_{\text{int}} = \frac{1}{3}\pi \frac{r_{\text{int}}^3}{K}.$$

We deduce that:

$$r_{\text{int}} = \left(\frac{3K}{\pi}\text{EP}_{\text{int}}\right)^{1/3} = \left(\frac{3K}{\pi}\text{EP}_{t-1}(e^{-\rho_{\text{evap}} S_{t-1}})\right)^{1/3}$$

The second phase concerns the rainwater trapping. Let P_t be the rainfall height between time $t-1$ and time t. The rainwater that comes into the tree hole is approximated by a cylinder $\pi R^2 P_t$. Because of infiltration, only a fraction $\theta_{\text{eff},t}$ of this water is trapped. $\theta_{\text{eff},t}$ depends on $\Delta S_{t-1,t}$, the normalized difference between the basis of the cone, πR^2, and the trapped water surface in the cone after evaporation, πr_{int}^2:

$$\Delta S_{t-1,t} = \frac{\pi R^2 - \pi r_{\text{int}}^2}{\pi R^2} = \frac{R^2 - r_{\text{int}}^2}{R^2}.$$

The bigger this surface, the more infiltration there is. Moreover, $\theta_{\text{eff},t}$ being a fraction, it is bounded between 0 and 1. So we express $\theta_{\text{eff},t}$ as:

$$\theta_{\text{eff},t} = e^{-\rho_{\text{eff}} \Delta S_{t-1,t}}, \quad \text{with } \rho_{\text{eff}} \geq 0.$$

After evaporation and rainwater trapping, the volume of water in the tree hole is:

$$\begin{aligned}\text{EP}_t &= \text{EP}_{\text{int}} + (\theta_{\text{eff},t} \times \pi R^2 P_t) \\ &= \text{EP}_{t-1}(1 - \theta_{\text{evap},t}) + (\theta_{\text{eff},t} \times \pi R^2 P_t).\end{aligned}$$

Finally, EP_t, the trapped water at time t, is bounded by the tree hole capacity $\text{EP}_{\max} = \pi \times R^2 \times (H/3)$. So, we obtain:

$$\text{EP}_t = \min((\text{EP}_{t-1}(1 - \theta_{\text{evap},t}) + \theta_{\text{eff},t}\pi R^2 P_t), \text{EP}_{\max}).$$

References

Agnew, P., Hide, M., Sidobre, C., Michalakis, Y., 2002. A minimalist approach to the effects of density-dependent competition on insect life-history traits. Ecol. Entomol. 27, 396–402.

Ahumada, J.A., Lapointe, D., Samuel, M.D., 2004. Modeling the population dynamics of *Culex quinquefasciatus* (Diptera: Culicidae), along an elevation gradient in Hawaii. J. Med. Entomol. 41, 1157–1170.

Awerbuch-Friedlander, T., Levins, R., Predescu, M., 2005. The role of seasonality in the dynamics of deer tick populations. Bull. Math. Biol. 67, 467–486.

Bommarco, R., 2001. Using matrix models to explore the influence of temperature on population growth of arthropod pests. Agric. Forest Entomol. 3, 275–283.

Caswell, H., 2001. Matrix Population Models: Construction, Analysis and Interpretation, second ed. Sinauer Ass. Inc. Publishers.

Chattopadhyay, J., Sarkar, R.R., Chaki, S., Bhattacharya, S., 2004. Effects of environmental fluctuations on the occurrence of malignant malaria—a model based study. Ecol. Model. 177, 179–192.

Chevalier, V., de la Rocque, S., Baldet, T., Vial, L., Roger, F., 2004. Epidemiological processes involved in the emergence of vector-borne diseases: West Nile fever, Rift Valley fever, Japanese encephalitis and Crimean-Congo haemorrhagic fever. Revue Scientifique Et Technique De L Office International Des Epizooties 23, 535–555.

Choi, W.I., Ryoo, M.I., 2003. A matrix model for predicting seasonal fluctuations in field populations of *Paronychiurus kimi* (Collembola: Onychiuridae). Ecol. Model. 162, 259–265.

Cordellier, R., 1978. Les vecteurs potentiels sauvages dans l'épidémiologie de la fièvre jaune en Afrique de l'Ouest. Travaux et documents ORSTOM, vol. 81, Paris, 1978, 258 pp.

Costantino, R.F., Cushing, J.M., Dennis, B., Desharnais, R.A., 1998. Resonant population cycles in temporally fluctuating habitats. Bull. Math. Biol. 60, 247–273.

Depinay, J.M.O., Mbogo, C.M., Killeen, G., Knols, B., Beier, J., Carlson, J., Dushoff, J., Billingsley, P., Mwambi, H., Githure, J., Toure, A.M., McKenzie, F.E., 2004. A simulation model of African Anopheles ecology and population dynamics for the analysis of malaria transmission. Malaria J. 3.

Derouich, M., Boutayeb, A., Twizell, E.H., 2003. A model of dengue fever. BioMed. Eng. Online 2, 4.

Esteva, L., Vargas, C., 1999. A model for dengue disease with variable human population. J. Math. Biol. 38, 220–240.

Focks, D.A., Haile, D.G., Daniels, E., Mount, G.A., 1993. Dynamic life table model for *Aedes-Aegypti* (Diptera, Culcidae)—analysis of the literature and model development. J. Med. Entomol. 30, 1003–1017.

Fouque, F., Baumgartner, J., 1996. Simulating development and survival of *Aedes vexans* (Diptera: Culicidae) preimaginal stages under field conditions. J. Med. Entomol. 33, 32–38.

Ghosh, M., Pugliese, A., 2004. Seasonal population dynamics of ticks, and its influence on infection transmission: a semi-discrete approach. Bull. Math. Biol. 66, 1659–1684.

Glass, K., 2005. Ecological mechanisms that promote arbovirus survival: a mathematical model of Ross River virus transmission. Trans. R. Soc. Trop. Med. Hyg. 99, 252–260.

Ishikawa, H., Ishii, A., Nagai, N., Ohmae, H., Harada, M., Suguri, S., Leafasia, J., 2003. A mathematical model for the transmission of *Plasmodium vivax* malaria. Parasitol. Int. 52, 81–93.

Jarry, M., Khaladi, M., Gouteux, J.P., 1996. A matrix model for studying tsetse fly populations. Entomol. Exp. Appl. 78, 51–60.

Jensen, A.L., 1995. Simple density-dependent matrix model for population projection. Ecol. Model. 77, 43–48.

Lord, C.C., 1998. Density dependence in larval *Aedes albopictus* (Diptera: Culicidae). J. Med. Entomol. 35, 825–829.

Lord, C.C., 2004. Seasonal population dynamics and behaviour of insects in models of vector-borne pathogens. Physiol. Entomol. 29, 214–222.

Mazaris, A.D., Matsinos, Y.G., 2006. An individual based model of sea turtles: Investigating the effect of temporal variability on population dynamics. Ecol. Model. 194, 114–124.

Mondet, B., 1994. Age physiologique et biologie des *Aedes* (Diptera: Culicidae) vecteurs potentiels de fièvre jaune en Côte d'Ivoire. Implications épidémiologiques. Thesis. Paris-Sud University.

Mondet, B., 1997. Importance of Aedes (Diceromyia) furcifer Edwards, 1913 (Diptera: Culicidae) among the arbovirus potential vectors, in the epidemiology of the yellow fever, in the sub-Sudanese savannas of Ivory Coast. Annales de la Societe Entomologique de France 33, 47–54.

Mondet, B., Montange, L., 1993. Presence of Aedes (Stegomyia) usambara Mattingly, 1953 (Diptera: Culicidae) in the Ivory Coast, seasonal variations

and epidemiological position. Annales de la Societe Entomologique de France 29, 261–267.

Moon, T.E., 1976. Astatistical model of the dynamics of a mosquito vector (*Culex tarsalis*) population. Biometrics 32, 355–368.

Ngwa, G.A., 2004. Modelling the dynamics of endemic malaria in growing populations. Dis. Cont. Dyn. Syst. Ser. B 4, 1173–1202.

Ngwa, G.A., Shu, W.S., 2000. A mathematical model for endemic malaria with variable human and mosquito populations. Math. Comput. Model. 32, 747–763.

Renshaw, M., Service, M.W., Birley, M.H., 1993. Density-dependent regulation of *Aedes-Cantans* (Diptera, Culicidae) in natural and artificial populations. Ecol. Entomol. 18, 223–233.

Shone, S.M., Curriero, F.C., Lesser, C.R., Glass, G.E., 2006. Characterizing population dynamics of *Aedes sollicitans* (Diptera: Culicidae) using meteorological data. J. Med. Entomol. 43, 393–402.

Teng, H.J., Apperson, C.S., 2000. Development and survival of immature *Aedes albopictus* and *Aedes triseriatus* (Diptera: Culicidae) in the laboratory: effects of density, food, and competition on response to temperature. J. Med. Entomol. 37, 40–52.

Thomas, L., Buckland, S.T., Newman, K.B., Harwood, J., 2005. A unified framework for modelling wildlife population dynamics. Aust. N. Z. J. Stat. 47, 19–34.

Tomori, O., 2004. Yellow fever: the recurring plague. Crit. Rev. Clin. Lab. Sci. 41, 391–427.